

BAYESIAN GENERATIONAL POPULATION-BASED TRAINING

Xingchen Wan¹, Cong Lu¹, Jack Parker-Holder¹, Philip J. Ball¹

Vu Nguyen², Binxin Ru¹, Michael A. Osborne¹

¹Machine Learning Research Group, University of Oxford, Oxford, UK

²Amazon, Adelaide, Australia

{xwan, conglu, jackph, ball, robin, mosb}@robots.ox.ac.uk, vu@ieee.org

ABSTRACT

Reinforcement learning (RL) offers the potential for training generally capable agents that can interact autonomously in the real world. However, one key limitation is the brittleness of RL algorithms to core hyperparameters and network architecture choice. Furthermore, non-stationarities such as evolving training data and increased agent complexity mean that different hyperparameters and architectures may be optimal at different points of training. This motivates AutoRL, a class of methods seeking to automate these design choices. One prominent class of AutoRL methods is Population-Based Training (PBT), which have led to impressive performance in several large scale settings. In this paper, we introduce two new innovations in PBT-style methods. First, we employ trust-region based Bayesian Optimization, enabling full coverage of the high-dimensional mixed hyperparameter search space. Second, we show that using a *generational* approach, we can also learn both architectures and hyperparameters jointly on-the-fly in a single training run. Leveraging the new highly parallelizable Brax physics engine, we show that these innovations lead to large performance gains, significantly outperforming the tuned baseline while learning entire configurations on the fly.

1 INTRODUCTION

Reinforcement Learning (RL) (Sutton & Barto, 2018) has proven to be a successful paradigm for training agents across a variety of domains and tasks (Mnih et al., 2013; Silver et al., 2017; Kalashnikov et al., 2018; Nguyen et al., 2021a), with some believing it could be enough for training generally capable agents (Silver et al., 2021). However, a crucial factor limiting the wider applicability of RL to new problems is the notorious sensitivity of algorithms with respect to their hyperparameters (Henderson et al., 2018; Andrychowicz et al., 2021; Engstrom et al., 2020), which often require expensive tuning. Indeed, it has been shown that when tuned effectively, good configurations often lead to dramatically improved performance in larger, more open-ended settings (Chen et al., 2018).

To address these challenges, recent work in *Automated Reinforcement Learning* (AutoRL, Parker-Holder et al. (2022)) has shown that rigorously searching these parameter spaces can lead to previously unseen levels of performance, even capable of breaking widely used simulators (Zhang et al., 2021). However, AutoRL contains unique challenges, as different tasks even in the same suite are often best solved with different network architectures and hyperparameters (Furuta et al., 2021; Xu et al., 2022). Furthermore, due to the non-stationarities present in RL (Igl et al., 2021), such as changing data distributions and the requirement for agents to model increasingly complex behaviors over time, optimal hyperparameters and architectures may not remain constant. To address this, works have shown adapting hyperparameters through time (Paul et al., 2019; Zhang et al., 2021; Parker-Holder et al., 2021; Jaderberg et al., 2017) and defining fixed network architecture schedules (Czarnecki et al., 2018) can be beneficial for performance. However, architectures and hyperparameters are inherently linked (Park et al., 2019), and to date, no method combines the ability to jointly and continuously adapt both on the fly.

In this paper we focus on Population-based Training (PBT) (Jaderberg et al., 2017) methods, where a population of agents is trained in parallel, copying across stronger weights and enabling adaption of

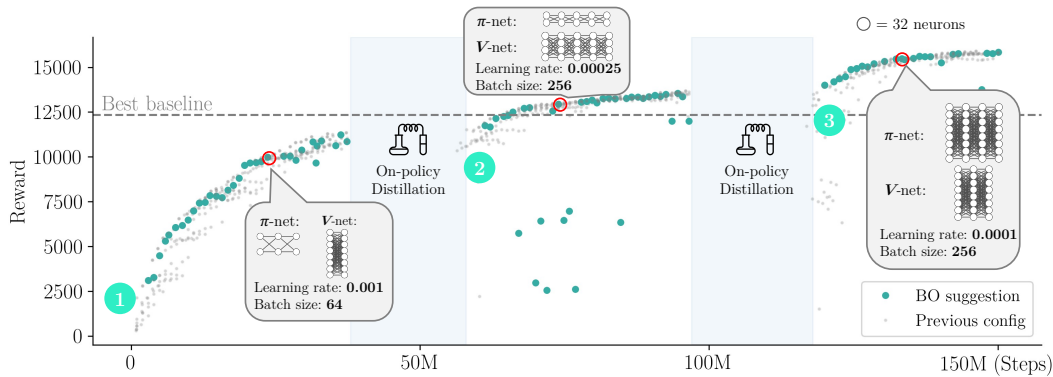


Figure 1: An example run of BG-PBT on the HalfCheetah task in BRAX: BG-PBT combines population-based training with high-dimensional Bayesian optimization, generational training (different generations marked with numbers in the figure) and on-policy distillation between generations to transfer across RL agents with different neural architectures: at different points during training, both hyperparameters and the architectures of policy & value networks are tuned on-the-fly, leading to significant improvement over the PPO baseline.

hyperparameters in a single training run. This allows PBT methods to achieve impressive performance on many large-scale settings (Jaderberg et al., 2019; Liu et al., 2021). However, PBT-style methods are typically limited in scope due to two key factors: 1) they only optimize a handful of hyperparameters, either due to using random search (Jaderberg et al., 2017), or model-based methods that do not scale to higher dimensions (Parker-Holder et al., 2020; 2021); 2) PBT methods are usually restricted to the same fixed architecture since weights are copied between agents.

We seek to overcome both of these issues in this paper, and propose *Bayesian Generational Population-based Training* (BG-PBT), with an example run demonstrated in Fig. 1. BG-PBT is capable of tuning a significantly greater proportion of the agent’s configuration, thanks to two new ideas. First, we introduce a new model-based *hyperparameter and architecture* exploration step motivated by recent advances in local Bayesian optimization (Wan et al., 2021). Second, we take inspiration from Stooke et al. (2021) who showed that PBT can be particularly effective when combined with network distillation (Igl et al., 2021), in an approach known as generational learning. As prior works in generational training (Vinyals et al., 2019; Stooke et al., 2021) show, the use of successive generations of architectures with distillation results in significantly reduced training time for new agents. This provides us with an algorithm-agnostic framework to create agents which continuously discover their *entire configuration*. Thus, for the first time, we can tune hyperparameters and architectures during one training run as part of a single unified algorithm.

We run a series of exhaustive experiments tuning both the architectures and hyperparameters for a Proximal Policy Optimization (PPO) (Schulman et al., 2017) agent in the newly introduced BRAX environment suite (Freeman et al., 2021). BRAX enables massively parallel simulation of agents, making it perfect for testing population-based methods without vast computational resources. Our agents significantly outperform both the tuned baseline and a series of prior PBT methods. Notably, we observe that BG-PBT often discovers a *schedule of networks* during training—which would be infeasible to train from scratch. We believe that given access to more compute, and a sufficiently challenging task, that BG-PBT is a significant step towards agents that never stop learning, as the hyperparameters and architecture search component makes the agent amenable to learning in open-ended environments. Furthermore, BG-PBT discovers entirely new modes of behavior for these representative environments, which we show at <https://sites.google.com/view/bgpbt>.

To summarize, the main contributions of this paper are as follows:

1. We show for the first time it is possible to select architectures as part of a PBT framework, using *generational training with policy distillation* with Neural Architecture Search (NAS).
2. We propose a novel and efficient algorithm, **BG-PBT**, especially designed for high-dimensional mixed search spaces, which can select both architectures and hyperparameters on-the-fly with provable efficiency guarantees.
3. We show in a series of experiments our *automatic architecture curricula* make it possible to achieve significantly higher performance than previous methods.

2 PRELIMINARIES

We begin by introducing the reinforcement learning framework, population-based training, which our method is based on, and the general problem setup we investigate in this paper.

Reinforcement Learning. We model the environment as a Markov Decision Process (MDP) (Sutton & Barto, 2018), defined as a tuple $M = (\mathcal{S}, \mathcal{A}, P, R, \rho_0, \gamma)$, where \mathcal{S} and \mathcal{A} denote the state and action spaces respectively, $P(s_{t+1}|s_t, a_t)$ the transition dynamics, $R(s_t, a_t)$ the reward function, ρ_0 the initial state distribution, and $\gamma \in (0, 1)$ the discount factor. The goal is to optimize a policy $\pi(a_t|s_t)$ that maximizes the expected discounted return $\mathbb{E}_{\pi, P, \rho_0} [\sum_{t=0}^{\infty} \gamma^t R(s_t, a_t)]$. Given a policy π , we may define the state value function $V^\pi(s) = \mathbb{E}_{\pi, P} [\sum_{t=0}^{\infty} \gamma^t R(s_t, a_t) | s_0 = s]$ and the state-action value-function $Q^\pi(s, a) = \mathbb{E}_{\pi, P} [\sum_{t=0}^{\infty} \gamma^t R(s_t, a_t) | s_0 = s, a_0 = a]$. The advantage function is then defined as the difference $A^\pi(s, a) = Q^\pi(s, a) - V^\pi(s)$.

A popular algorithm for online continuous control that we use is PPO (Schulman et al., 2017). PPO achieves state-of-the-art results for popular benchmarks (Cobbe et al., 2020) and is hugely parallelizable, making it an ideal candidate for population-based methods (Parker-Holder et al., 2020). PPO approximates TRPO (Schulman et al., 2015) and uses a clipped objective to stabilize training:

$$\mathcal{L}_{\text{PPO}}(\theta) = \min \left(\frac{\pi_\theta(a|s)}{\pi_\mu(a|s)} A^{\pi_\mu}, g(\theta, \mu) A^{\pi_\mu} \right), \text{ where } g(\theta, \mu) = \text{clip} \left(\frac{\pi_\theta(a|s)}{\pi_\mu(a|s)}, 1 - \epsilon, 1 + \epsilon \right) \quad (1)$$

where π_μ is a previous policy and ϵ is the clipping parameter.

Population-Based Training. RL algorithms, including PPO, are typically quite sensitive to their hyperparameters. PBT (Jaderberg et al., 2017) is an evolutionary method that tunes RL hyperparameters on-the-fly. It optimizes a population of B agents in parallel, so that their weights and hyperparameters may be dynamically adapted within a single training run. In the standard paradigm without architecture search, we consider two sub-routines, explore and exploit. We train for a total of T steps and evaluate performance every $t_{\text{ready}} < T$ steps. In the exploit step, the weights of the worst-performing agents are replaced by those from an agent randomly sampled from the set of best-performing ones, via *truncation selection*. To select new hyperparameters, we perform the explore step. We denote the hyperparameters for the b th agent in a population at timestep t as $\mathbf{z}_t^b \in \mathcal{Z}$; this defines a *schedule* of hyperparameters over time $(\mathbf{z}_t^b)_{t=1, \dots, T}$. Let $f_t(\mathbf{z}_t)$ be an objective function (e.g. the return of a RL agent) under a given set of hyperparameters at timestep t , our goal is to maximize the final performance $f_T(\mathbf{z}_T)$. The original PBT uses a combination of random sampling and evolutionary search for the explore step by suggesting new hyperparameters mutated from the best-performing agents. Population Based Bandit (PB2) and PB2-Mix (Parker-Holder et al., 2020; 2021) improve on PBT by using *Bayesian optimization* (BO) to suggest new hyperparameters, relying on a time-varying *Gaussian Process* (GP) (Rasmussen & Williams, 2006) to model the data observed. We will also use GP-based BO in our method, and we include a primer of GPs and BO in App. A.

Problem Setup. We follow the notation used in Parker-Holder et al. (2020) and frame the hyperparameter optimization problem in the lens of optimizing an expensive, time-varying, black-box reward function $f_t : \mathcal{Z} \rightarrow \mathbb{R}$. Every t_{ready} steps, we observe and record noisy observations, $y_t = f_t(\mathbf{z}_t) + \epsilon_t$, where $\epsilon_t \sim \mathcal{N}(0, \sigma^2 \mathbf{I})$ for some fixed variance σ^2 . We follow the typical PBT setup by defining a hyperparameter space, \mathcal{Z} , which for the BRAX (Freeman et al., 2021) implementation of PPO we follow in the paper, consists of 9 parameters: learning rate, discount factor (γ), entropy coefficient (c), unroll length, reward scaling, batch size, updates per epoch, GAE parameter (λ) and clipping parameter (ϵ). To incorporate the architecture hyperparameters, $\mathbf{y} \in \mathcal{Y}$, we add 6 additional parameters leading to a 15-dimensional joint space $\mathcal{J} = \mathcal{Y} \times \mathcal{Z}$. For both the policy and value networks, we add the width and depth of the Multi-layer Perceptron (MLP) and a binary flag on whether to use spectral normalization.

3 BAYESIAN GENERATIONAL POPULATION-BASED TRAINING (BG-PBT)

We present BG-PBT in Algorithm 1 which consists of two major components. First, a BO approach to select new hyperparameter configurations \mathbf{z} for our agents (§3.1). We then extend the search space to accommodate architecture search, allowing agents to choose their own networks (parameterized by $\mathbf{y} \in \mathcal{Y}$) and use on-policy distillation to transfer between different architectures (§3.2).

3.1 HIGH-DIMENSIONAL BO AGENTS IN MIXED-INPUT CONFIGURATION SPACE FOR PBT

Existing population-based methods ignore (PB2) or only partially address (PB2-Mix, which does not consider ordinal variables such as integers) the heterogeneous nature of the mixed hyperparameter space \mathcal{Z} . Furthermore, both previous methods are equipped with standard GP surrogates which typically scale poorly beyond low-dimensional search spaces, and are thus only used to tune a few selected hyperparameters deemed to be the most important based on human expertise. To address these issues, BG-PBT explicitly accounts for the characteristics of typical RL hyperparameter search space by making several novel extensions to CASMOPOLITAN (Wan et al., 2021), a state-of-the-art BO method for high-dimensional, mixed-input problems for our setting. In this section, we outline the main elements of our design, and we refer the reader to App. B.2 for full technical details of the approach.

Tailored treatment of mixed hyperparameter types.

Hyperparameters in RL can be continuous (e.g. discounting factor), ordinal (discrete variables with ordering, e.g. batch size) and categorical (discrete variables without ordering, e.g. activation function). BG-PBT treats each variable type differently: we use tailored kernels for the GP surrogate, and utilize interleaved optimization for the acquisition function, alternating between local search for the categorical/ordinal variables and gradient descent for the continuous variables. BG-PBT extends both CASMOPOLITAN and PB2-Mix by further accommodating ordinal variables, as both previous works only considered continuous and categorical variables.

Trust Regions (TR). TRs have proven success in extending GP-based BO to higher-dimensional search spaces, which were previously intractable due to the curse of dimensionality, by limiting exploration to promising regions in the search space based on past observations (Eriksson et al., 2019; Wan et al., 2021). In the PBT context, TRs also implicitly avoid large jumps in hyperparameters, which improves training stability. We adapt the TRs used in the original CASMOPOLITAN to the time-varying setup by defining TRs around the current best configuration, and then adjusting them dynamically: similar to Eriksson et al. (2019) and Wan et al. (2021), TRs are expanded or shrunk upon consecutive “successes” or “failures”. We define a proposed configuration to be a “success” if it appears in the top $q\%$ -performing agents and a “failure” otherwise. When the TRs shrink below some specified minimum, a *restart* is triggered, which resets the GP surrogate to avoid becoming stuck at a local optimum. We adapt the Upper Confidence Bound (UCB)-based criterion proposed in Wan et al. (2021) which is based on a global, auxiliary GP model to the time-varying setting to re-initialize the population when a restart is triggered. Full details are provided in App. B.4.

Theoretical Properties. Following Wan et al. (2021), we show that under typical assumptions (presented in App. C) used for TR-based algorithms (Yuan, 1999), our proposed BG-PBT converges to the global optimum asymptotically. Furthermore, we derive an upper bound on the cumulative regret and show that under certain conditions it achieves sublinear regret. We split the search space into $\mathcal{Z} = [\mathcal{H}, \mathcal{X}]$ (categorical/continuous parts respectively). We note that Assumption C.3 considers the minimum TR lengths L_{\min}^x, L_{\min}^h are set to be small enough so that the GP approximates f accurately in the TRs. In practice, this assumption only holds asymptotically, i.e. when the observed datapoints in the TRs goes to infinity. We present the main result, the time-varying extension to Theorem 3.4 from Wan et al. (2021), and then refer to App. C for the derivation.

Algorithm 1 BG-PBT; distillation and NAS steps marked in magenta (§3.2)

- 1: **Input:** pop size B , t_{ready} , max steps T , q (% agents replaced per iteration)
 - 2: **Initialize** B agents with weights $\{\theta_0^{(i)}\}_{i=1}^B$, random hyperparameters $\{\mathbf{z}_0^{(i)}\}_{i=1}^B$ and architectures $\{\mathbf{y}_0^{(i)}\}_{i=1}^B$,
 - 3: **for** $t = 1, \dots, T$ (in parallel for all B agents) **do**
 - 4: Train models & record data for all agents
 - 5: **if** $t \bmod t_{\text{ready}} = 0$ **then**
 - 6: Replace the weights & architectures of the bottom $q\%$ agents with those of the top $q\%$ agents.
 - 7: Update the surrogate with new observations & rewards and adjust/restart the trust regions.
 - 8: Check whether to start a new generation (see §3.2).
 - 9: **if** start a new generation **then**
 - 10: Clear the GP training data.
 - 11: Create B agents with archs. from BO/random.
 - 12: Distill from a top- $q\%$ performing agent of the existing generation to new agents.
 - 13: **else**
 - 14: Select new hyperparameters \mathbf{z} for the agents whose weights have been just replaced with randomly sampled configs (if $\mathbf{D} = \emptyset$) **OR** using the suggestions from the BO agent described conditioned on \mathbf{y} (otherwise).
-

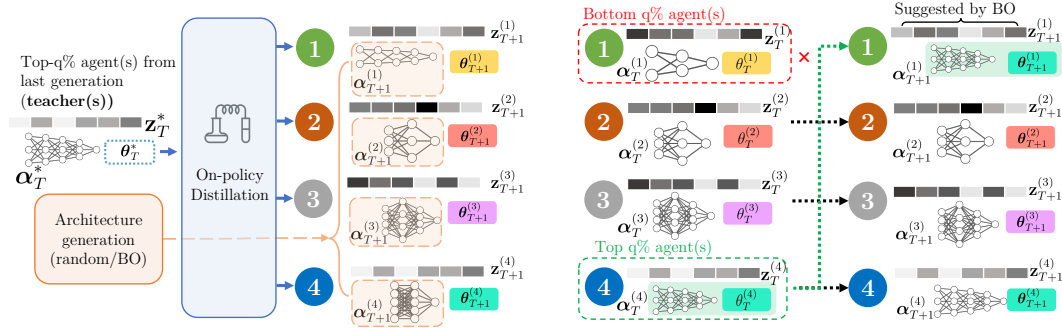


Figure 2: BG-PBT (a) at the *beginning* of a generation (left) and (b) *during* a generation (right). At the start of a generation, agents with diverse architectures are suggested and on-policy distillation is used to transfer information across generations & different architectures (§3.2). Within a generation, a high-dimensional, mixed-input BO agent suggests hyperparameters (§3.1, we copy weights across fixed architectures).

Theorem 3.1. Assume Assumptions C.2 & C.3 hold. Let $f_i : [\mathcal{H}, \mathcal{X}] \rightarrow \mathbb{R}$ be a time-varying objective defined over a mixed space and $\zeta \in (0, 1)$. Suppose that: (i) there exists a class of functions g_i in the RKHS $\mathcal{G}_k([\mathcal{H}, \mathcal{X}])$ corresponding to the kernel k of the global GP model, such that g_i passes through all the local maximas of f_i and shares the same global maximum as f_i ; (ii) the noise at each timestep ϵ_i has mean zero conditioned on the history and is bounded by σ ; (iii) $\|g_i\|_k^2 \leq B$. Then BG-PBT obtains a regret bound

$$\Pr\left\{R_{IB} \leq \sqrt{\frac{C_1 I \beta_I}{B}} \gamma(IB; k; [\mathcal{H}, \mathcal{X}]) + 2 \quad \forall I \geq 1\right\} \geq 1 - \zeta,$$

with $C_1 = 8/\log(1 + \sigma^{-2})$, $\gamma(T; k; [\mathcal{H}, \mathcal{X}])$ defined in Theorem C.1 and β_I is parameter balancing exploration-exploitation as in Theorem 2 of Parker-Holder et al. (2020).

Under the same ideal conditions assumed in Bogunovic et al. (2016); Parker-Holder et al. (2020) where the objective does not vary significantly through time, the cumulative regret bound is sublinear with $\lim_{I \rightarrow \infty} \frac{R_{IB}}{I} = 0$, when $\omega \rightarrow 0$ and $\tilde{N} \rightarrow I$.

3.2 ADAPTING ARCHITECTURES ON THE FLY

Now that we are equipped with an approach to optimize in high-dimensional \mathcal{Z} , we focus on choosing *network architectures*. Despite their importance in RL (Cobbe et al., 2019; Furuta et al., 2021), architectures remain underexplored as a research direction. Adapting architectures for PBT methods is non-trivial as we further enlarge the search space, and weights cannot readily be copied across different networks. Inspired by Stooke et al. (2021), our key idea is that when beginning a new *generation* we can distill behaviors into new architectures (see Fig. 2). Specifically:

- *Starting each generation:* We fill the population of B agents by generating a diverse set of architectures for both the policy and value networks. For the first generation, this is done via random sampling. For subsequent generations, we use suggestions from BO and/or random search with successive halving over the architecture space \mathcal{Y} only; the BO is trained on observations of the best performance each architecture has achieved in previous generations. We initialize a new generation when the evaluated return stagnates beyond a pre-set patience during training.
- *Transfer between generations:* Apart from the very first generation, we transfer information from the best agent(s) of the previous generation to each new agent, in a similar fashion to Stooke et al. (2021), using on-policy distillation with a joint supervised and RL loss between *different architectures* as shown in Fig. 2a. Given a learned policy π_i and value function V_i from a previous generation, the new joint loss optimized is:

$$\mathbb{E}_{(s_t, a_t) \sim \pi_{i+1}} [\alpha_{\text{RL}} \mathcal{L}_{\text{RL}} + \alpha_V \|V_i(s_t) - V_{i+1}(s_t)\|_2 + \alpha_\pi \mathbb{D}_{\text{KL}}(\pi_i(\cdot | s_t) || \pi_{i+1}(\cdot | s_t))] \quad (2)$$

for weights $\alpha_{\text{RL}} \geq 0$, $\alpha_V \geq 0$, $\alpha_\pi \geq 0$, and RL loss \mathcal{L}_{RL} taken from Equation (1). We linearly anneal the supervised losses over the course of each generation, so that by the end, only the RL loss remains.

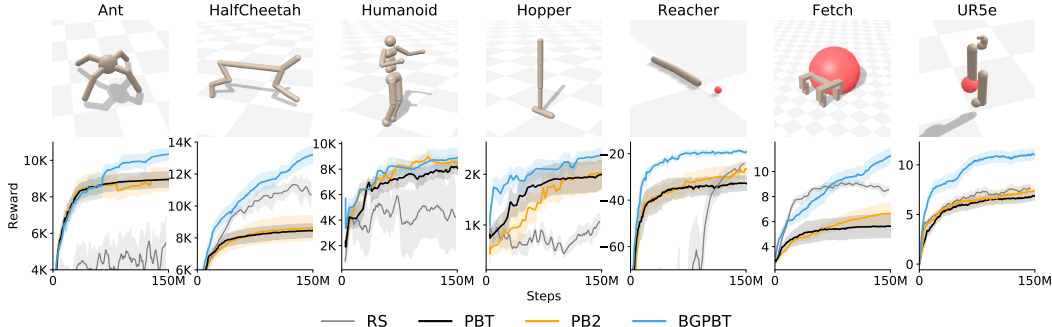


Figure 3: Visualization of each environment (**top row**) and mean evaluated return over the population with ± 1 SEM (shaded) across 7 random seeds (**bottom row**) in all environments. RS refers to the higher performing of RS- \mathcal{Z} or RS- \mathcal{J} in Table 1.

Table 1: Mean evaluated return ± 1 SEM across 7 seeds shown. For PBT-style methods (PBT, PB2 and BG-PBT), the mean best-performing agent in the population is shown. Methods performing within 1 SEM of the best-performing method are bolded (the same applies to all tables).

Method	PPO*	RS	RS	PBT	PB2	BG-PBT
Search space	\mathcal{Z}	\mathcal{Z}	\mathcal{J}	\mathcal{Z}	\mathcal{Z}	\mathcal{J}
Ant	3853 ± 676	6780 ± 317	4781 ± 515	8955 ± 385	8954 ± 594	10349 ± 326
HalfCheetah	6037 ± 236	9502 ± 76	10340 ± 329	8455 ± 400	8629 ± 746	13216 ± 503
Humanoid	9109 ± 987	4004 ± 519	4652 ± 1002	7954 ± 437	8452 ± 512	8894 ± 716
Hopper	120 ± 43	339 ± 25	943 ± 185	2002 ± 254	2027 ± 323	2381 ± 127
Fetch	14.0 ± 0.2	5.2 ± 0.4	8.6 ± 0.2	5.5 ± 0.8	6.6 ± 0.7	11.3 ± 0.6
Reacher	-189.3 ± 43.7	-24.2 ± 1.4	-95.2 ± 25.3	-32.9 ± 2.8	-26.6 ± 2.6	-19.2 ± 0.9
UR5e	5.2 ± 0.2	5.3 ± 0.4	7.7 ± 0.3	6.9 ± 0.4	7.4 ± 0.6	11.0 ± 0.5

*From the BRAX authors and implemented in a different framework (JAX) to ours (PyTorch)

- *During a generation:* We follow standard PBT methods to evolve the hyperparameters of each agent by copying weights θ and the architecture y from a top- $q\%$ performing agent to a bottom- $q\%$ agent, as shown in Fig. 2b. This creates an effect similar to successive halving (Karnin et al., 2013; Jamieson & Talwalkar, 2016) where poorly-performing architectures are quickly removed from the population in favor of more strongly-performing ones; typically at the end of a generation, 1 or 2 architectures dominate the population. While we do not introduce new architectures within a generation, the hyperparameter suggestions are conditioned on the current policy and value architectures by incorporating the architecture parameters y as contextual fixed dimensions in the GP surrogate described in §3.1.

4 EXPERIMENTS

While BG-PBT provides a framework applicable to any RL algorithm, we test our method on 7 environments from the new BRAX environment suite, using PPO. We begin by presenting a comparative evaluation of BG-PBT against standard baselines in population-based training to both show the benefit of searching over the full hyperparameter space with local BO and of automatically adapting architectures over time. We further show that our method beats end-to-end BO, showing the advantage of dynamic schedules. Next, we analyze these learned hyperparameter and architecture schedules using BG-PBT and we show analogies to similar trends in learning rate and batch size in supervised learning. Finally, we perform ablations on individual components of BG-PBT. For all population-based methods, we use a population size $B = 8$ and a total budget of 150M steps. We note that BG-PBT with NAS uses additional on-policy samples from the environment in order to distill between architectures. We instantiate the BRAX environments with an action repeat of 1. We use t_{ready} of 1M for all PBT-based methods on all environments except for Humanoid and Hopper, where we linearly anneal t_{ready} from 5M to 1M. The remaining hyperparameters and implementation details used in this section are listed in App. E.

Comparative evaluation of BG-PBT. We first perform a comparative evaluation of BG-PBT against standard baselines in PBT-methods and the PPO baseline provided by the BRAX authors. We show the benefit of using local BO and treating the whole RL hyperparameter space \mathcal{Z} , by comparing BG-PBT against PBT (Jaderberg et al., 2017), PB2 (Parker-Holder et al., 2020) and Random Search (RS) using the default architecture in BRAX. In RS, we simply sample from the hyperparameter space

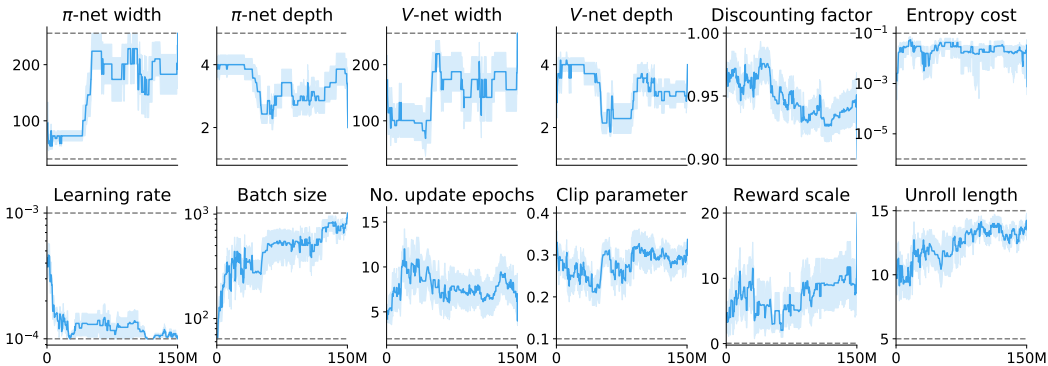
Table 2: Comparison against sequential BO*

Method	BO- \mathcal{Z} *	BO- \mathcal{J} *	BG-PBT
Ant	6975 \pm 1013	7149 \pm 507	10349\pm326
HalfCheetah	11202 \pm 204	10859 \pm 174	13216\pm503
Humanoid	9040\pm1303	4845 \pm 962	8894\pm716
Hopper	358 \pm 60	1254 \pm 154	2381\pm127
Fetch	13.2\pm0.2	11.6 \pm 0.1	11.3 \pm 0.6
Reacher	-17.3\pm0.3	-51.7 \pm 18.3	-19.2 \pm 0.9
UR5e	9.0 \pm 0.5	6.3 \pm 1.4	11.0\pm0.5

*More resources required compared to BG-PBT.

Table 3: Ablation studies

Method	No TR/NAS	No NAS	BG-PBT
Ant	8954 \pm 594	9352 \pm 402	10349\pm326
HalfCheetah	8629 \pm 746	9483 \pm 626	13216\pm503
Humanoid	8452 \pm 512	10359\pm647	8894 \pm 716
Hopper	2027 \pm 323	2511\pm154	2381\pm127
Fetch	6.6 \pm 0.7	7.3 \pm 0.8	11.3\pm0.6
Reacher	-26.6 \pm 2.6	-17.6\pm0.8	-19.2 \pm 0.9
UR5e	7.4 \pm 0.6	9.0 \pm 0.8	11.0\pm0.5

Figure 4: The hyperparameter and architecture schedule discovered by BG-PBT on Ant: we plot the hyperparameters of the best-performing agent in the population averaged across 7 seeds with ± 1 SEM shaded. Gray dashed lines denote the hyperparameter bounds.

and take the best performance found using the same compute budget as the PBT methods. Next, we include architecture search into BG-PBT using the full space \mathcal{J} and show significant gains in performance compared to BG-PBT without architectures; we use random search over \mathcal{J} as a baseline. The optimized PPO implementation from the BRAX authors is provided as a sequential baseline. We present the results in Table 1 and the training trajectories in Fig. 3.

We show that BG-PBT significantly outperforms the RS baselines and the existing PBT-style methods in almost all environments considered. We also observe that RS is a surprisingly strong baseline, performing on par or better than PBT and PB2 in HalfCheetah, Reacher, Fetch and UR5e — this is due to a well-known failure mode in PBT-style algorithms where they may be overly greedy in copying sub-optimal behaviors early on and then fail to sufficiently explore in weight space when the population size is modest. BG-PBT avoids this problem by *re-initializing networks each generation* and distilling, which prevents collapse to suboptimal points in weight space.

Comparison against sequential BO. We further compare against BO in the traditional sequential setup (Table 2): for each BO iteration, the agent is trained for the full 150M timesteps before a new hyperparameter suggestion is made. To enable BO to improve on RS, we allocate a budget of 50 evaluations, *which is approx. $6\times$ more expensive* than our method and up to $50\times$ more costly in terms of wall-clock time if vanilla, non-parallel BO is used. We implement this baseline using SMAC3 (Lindauer et al., 2022) in both the \mathcal{Z} and \mathcal{J} search spaces (denoted BO- \mathcal{Z} and BO- \mathcal{J} respectively in Table 2). While, unsurprisingly, BO improves over the RS baseline, BG-PBT still outperforms it in a majority of environments. One reason for this is that BG-PBT naturally discovers a dynamic schedule of hyperparameters and architectures, which is strictly more flexible than a carefully tuned but still static configuration – we analyze this below.

Analysis of discovered hyperparameter and architecture schedules. We present the hyperparameter and architecture schedules learned by BG-PBT in our main comparative evaluation on Ant in Fig. 4. We find consistent trends across environments such as the decrease of learning rate and increase in batch sizes over time, consistent to common practices in both RL (Engstrom et al., 2020) and supervised learning, but crucially BG-PBT discovers the same *without any pre-defined schedule*. We also find that different networks are favored at different stages of training, but the exact patterns differ across environments: for Ant (Fig. 4), we find that larger networks are preferred towards the end of training, with the policy and value network widths increasing over time: Prior work has shown that larger networks like those we automatically find towards the end of training *can be notoriously unstable and difficult to train from scratch* (Czarnecki et al., 2018; Ota et al., 2021), which further supports our use of generational training to facilitate this.

Ablation Studies. BG-PBT improves on existing methods by using local TR-based BO (§3.1) and NAS & distillation (§3.2). We conduct an ablation study by removing either or both components in Table 3, where “No NAS” does not search architectures or distill but uses the default BRAX architectures, and “No TR/NAS” further only uses a vanilla GP surrogate and is identical to PB2. We find the tailored BO agent in §3.1 improves performance across the board. On the importance of NAS & distillation, in all environments except for Humanoid and Reacher, BG-PBT matches or outperforms “No NAS”, despite \mathcal{J} being a more complicated search space and the “No NAS” baseline is conditioned on strongly-performing default architectures. We also see a particularly large gain for HalfCheetah and Fetch when we include architectures, demonstrating the effectiveness of the generational training and NAS in our approach.

5 RELATED WORK

On-the-fly hyperparameter tuning. Our work improves on previous PBT (Parker-Holder et al., 2020; Jaderberg et al., 2017; Zhang et al., 2021) style methods. In particular, we build upon Parker-Holder et al. (2021), using a more scalable BO step, and adding architecture search with generational learning. Dalibard & Jaderberg (2021) introduce an approach for increasing diversity in the weight space for PBT, orthogonal to our work. There have also been non-population-based methods for dynamic hyperparameter optimization, using bandits (Badia et al., 2020; Moskovitz et al., 2021; Parker-Holder et al., 2020; Ball et al., 2020), gradients (Paul et al., 2019; Xu et al., 2018; Zahavy et al., 2020; Flennerhag et al., 2021) or Evolution (Tang & Choromanski, 2020). Crucially, none of the methods described searches over architectures.

Architecture search. In RL, Czarnecki et al. (2018) showed increasing agent complexity over time could be effective, albeit with a pre-defined schedule. Miao et al. (2021) showed that DARTS (Liu et al., 2019) could be effective in RL, finding high performing architectures on the Procgen benchmark. Auto-Agent-Distiller (Fu et al., 2020) deals with the problem of finding optimal architectures for compressing the model size of RL agents, and also find that using distillation between the teacher and student networks improves stability of NAS in RL. BO has been used as a powerful tool for searching over large architecture spaces (Wan et al., 2021; Kandasamy et al., 2018; Ru et al., 2021; White et al., 2021; Nguyen et al., 2021b; Wan et al., 2022). Conversely, we only consider simple MLPs and the use of spectral normalization. There has been initial effort (Izquierdo et al., 2021) combining NAS and hyperparameter optimization in sequential settings, which is distinct to our on-the-fly approach.

Generational training and distillation. Stooke et al. (2021) recently introduced generational training, using policy distillation to transfer knowledge between generations, accelerating training. Our method is based on this idea, with changing generations. The use of distillation is further supported by Igl et al. (2021) who recently used this successfully to adapt to non-stationarities in reinforcement learning, however keeping hyperparameters and architectures fixed.

6 CONCLUSION & DISCUSSION

In this paper, we propose BG-PBT: a new algorithm that significantly increases the capabilities of PBT methods for RL. Using recent advances in Bayesian Optimization, BG-PBT is capable of searching over drastically larger search spaces than previous methods. Additionally, inspired by recent advances in generational learning, we show it is also possible to efficiently learn architectures on the fly as part of a unified algorithm. The resulting method leads to significant performance gains across the entire BRAX environment suite, achieving high performance even in previously untested environments, and is able to successfully handle non-stationarities present in RL (Igl et al., 2021).

We therefore believe that BG-PBT is a significant step towards training RL agents in open-endedness. Indeed, for this to be possible it is crucial that agents never stop learning, which may require them continuously expand and adapt their capabilities and architectures over time. For future work, we would be interested in testing BG-PBT in more open-ended environments, for example using an environment adversary to propose new challenges (Dennis et al., 2020; Jiang et al., 2021; Wang et al., 2019; 2020). Furthermore, with more agents in the population, we could even envision scaling up BG-PBT to dynamically adapt more aspects of an RL agent, including the update rules (Oh et al., 2020) or the entire algorithm (Co-Reyes et al., 2021).

A PRIMER ON GPs AND BO

Gaussian Processes In Bayesian Optimization (BO), Gaussian Processes, or GPs, act as *surrogate models* for a black-box function f which takes an input \mathbf{z} (in our case, the hyperparameters and/or the architecture parameters) and returns an output $y = f(\mathbf{z}) + \epsilon$ where $\epsilon \sim \mathcal{N}(0, \sigma^2)$. A GP defines a probability distribution over functions f under the assumption that any finite subset $\{(\mathbf{z}_i, f(\mathbf{z}_i))\}$ follows a normal distribution (Rasmussen & Williams, 2006). Formally, a GP is denoted as $f(\mathbf{z}) \sim \text{GP}(m(\mathbf{z}), k(\mathbf{z}, \mathbf{z}'))$, where $m(\mathbf{z})$ and $k(\mathbf{z}, \mathbf{z}')$ are called the mean and covariance functions respectively, i.e. $m(\mathbf{z}) = \mathbb{E}[f(\mathbf{z})]$ and $k(\mathbf{z}, \mathbf{z}') = \mathbb{E}[(f(\mathbf{z}) - m(\mathbf{z}))(f(\mathbf{z}') - m(\mathbf{z}'))^T]$. The covariance function (kernel) $k(\mathbf{z}, \mathbf{z}')$ can be thought of as a similarity measure relating $f(\mathbf{z})$ and $f(\mathbf{z}')$. There have been various proposed kernels which encode different prior beliefs about the function $f(\mathbf{z})$ (Rasmussen & Williams, 2006).

If we assume a zero mean prior $m(\mathbf{z}) = 0$, to predict $f_* = f(\mathbf{z}_*)$ at a new data point \mathbf{z}_* , we have,

$$\begin{bmatrix} \mathbf{f} \\ f_* \end{bmatrix} \sim \mathcal{N}\left(0, \begin{bmatrix} \mathbf{K} & \mathbf{k}_*^T \\ \mathbf{k}_* & k_{**} \end{bmatrix}\right), \quad (3)$$

where $k_{**} = k(\mathbf{z}_*, \mathbf{z}_*)$, $\mathbf{k}_* = [k(\mathbf{z}_*, \mathbf{z}_i)]_{\forall i \leq N}$, N is the number of observed points for the GP, and $\mathbf{K} = [k(\mathbf{z}_i, \mathbf{z}_j)]_{\forall i, j \leq N}$. Combining Eq. (3) with the fact that $p(f_* | \mathbf{f})$ follows a univariate Gaussian distribution $\mathcal{N}(\mu(\mathbf{z}_*), \sigma^2(\mathbf{z}_*))$, assuming we have observed $\{\mathbf{z}_1, f_1\}, \{\mathbf{z}_2, f_2\}, \dots, \{\mathbf{z}_t, f_t\}$ and collected all past reward observations as $\mathbf{f}_t = [f_1, \dots, f_t]^\top$, to predict the reward at a new configuration \mathbf{z}' , the GP posterior mean and variance at \mathbf{z}' can be computed as:

$$\mu_t(\mathbf{z}') := \mathbf{k}_t(\mathbf{z}')^T (\mathbf{K}_t + \sigma^2 \mathbf{I})^{-1} \mathbf{f}_t \quad (4)$$

$$\sigma_t^2(\mathbf{z}') := k(\mathbf{z}', \mathbf{z}') - \mathbf{k}_t(\mathbf{z}')^T (\mathbf{K}_t + \sigma^2 \mathbf{I})^{-1} \mathbf{k}_t(\mathbf{z}'), \quad (5)$$

where $\mathbf{K}_t := \{k(z_i, z_j)\}_{i, j=1}^t$ and $\mathbf{k}_t := \{k(z_i, z'_t)\}_{i=1}^t$.

Bayesian Optimization Bayesian optimization (BO) is a powerful sequential approach to find the global optimum of an expensive black-box function $f(\mathbf{z})$ without making use of derivatives. First, a surrogate model (in our case, a GP as discussed above) is learned from the current observed data $\mathcal{D}_t = \{\mathbf{z}_i, y_i\}_{i=1}^t$ to approximate the behavior of $f(\mathbf{z})$. Second, an *acquisition function* is derived from the surrogate model to select new data points that maximizes information about the global optimum – a common acquisition function that we use in our paper is the Upper Confidence Bound (UCB) (Srinivas et al., 2010) criterion which balances exploitation and exploration. Specifically, the UCB on a new, unobserved point \mathbf{z}' is given by:

$$\text{UCB}(\mathbf{z}') = \mu_t(\mathbf{z}') + \sqrt{\beta_t \sigma_t(\mathbf{z}')}, \quad (6)$$

where μ_t and σ_t are the posterior mean and standard deviation given in Eq. 4 above and $\beta_t > 0$ is a trade-off parameter between mean and variance. At each BO iteration, we find a batch of samples that sequentially maximizes the acquisition function above. The process is conducted iteratively until the evaluation budget is depleted, and the global optimum is estimated based on all the sampled data. In-depth discussions about BO beyond this brief overview can be found in recent surveys (Brochu et al., 2010; Shahriari et al., 2016; Frazier, 2018).

B BAYESIAN OPTIMIZATION FOR PBT

In this section, we provide specific details for the modifications to CASMOPOLITAN to make it amenable for our setup which consists of non-stationary reward and a mixed, high-dimensional search space.

B.1 KERNEL DESIGN

We use the following time-varying kernel (Parker-Holder et al., 2021) to measure the spatiotemporal distance between a pair of configuration vectors $\{\mathbf{z}, \mathbf{z}'\}$ with continuous, ordinal and/or categorical

dimensions, and whose rewards are observed at timesteps $\{i, j\}$. For the most general case where all three types of variables are involved, we have the following kernel function:

$$k(\mathbf{z}, \mathbf{z}', i, j) = \frac{1}{2} \left((k_x(\mathbf{x}, \mathbf{x}') + k_h(\mathbf{h}, \mathbf{h}')) + (k_x(\mathbf{x}, \mathbf{x}')k_h(\mathbf{h}, \mathbf{h}')) \right) \left((1 - \omega)^{|i-j|/2} \right) \quad (7)$$

where \mathbf{x} denotes the continuous *and ordinal* dimensions and \mathbf{h} denotes the categorical dimensions of the configuration vector \mathbf{z} , respectively, $k_x(\cdot, \cdot)$ is the kernel for continuous and ordinal inputs (by default Matérn 5/2), $k_h(\cdot, \cdot)$ is the kernel for the categorical dimensions (by default the exponentiated overlap kernel in Wan et al. (2021)) and $\omega \in [0, 1]$ controls how quickly old data is decayed and is learned jointly during optimization of the GP log-likelihood. When the search space only contains continuous/ordinal variables, we simply have $k(\mathbf{z}, \mathbf{z}', i, j) = k_x(\mathbf{x}, \mathbf{x}')(1 - \omega)^{|i-j|/2}$, and a similar simplification holds if the search space only contains categorical variables. We improve on Parker-Holder et al. (2021) by directly supporting ordinal variables such as integers (for e.g. batch size) and selecting them alongside categorical variables using *interleaved acquisition optimization* as opposed to time-varying bandits which scales poorly to large discrete spaces.

B.2 PROPOSING NEW CONFIGURATIONS

As discussed in App. A, a BO agent selects new configurations by selecting configuration(s) which maximize the acquisition function (in this case, the UCB acquisition function). This is typically achieved via off-the-shelf first-order optimizers, which is challenging in a mixed-input space as the discrete (ordinal and categorical) variables lack gradients and naïvely casting them into continuous variables yields invalid solutions which require rounding. To address this issue, Parker-Holder et al. (2021) select \mathbf{h} first via time-varying bandits (using the proposed TV.EXP3.M algorithm) and then select \mathbf{x} by optimizing the BO acquisition function, *conditioned on* the chosen \mathbf{h} . This method scales poorly to spaces with a large number of categorical choices, as bandit problems generally require pulling each arm at least once. Instead, we develop upon *interleaved acquisition optimization* introduced in Wan et al. (2021) which unifies all variables under a single GP, and alternates between optimization of the continuous and discrete variables:

Algorithm 2 Interleaved optimization of $\text{acq}(\mathbf{z})$

- 1: **while** not converged **do**
 - 2: **Continuous:** Do a single step of gradient descent on the continuous dimensions.
 - 3: **Ordinal and Categorical:** Conditioned on the new continuous values, do a single step of local search: randomly select an ordinal/categorical variable and choose a different (categorical), or an adjacent (ordinal) value, if the new value leads to an improvement in $\text{acq}(\cdot)$.
-

Compared to the approach in Wan et al. (2021), we include ordinal variables, which are optimized alongside the categorical variables via local search during acquisition optimization but are treated like continuous variables by the kernel. During acquisition, we define adjacent ordinals to be the neighboring values. For example, for an integer variable with a valid range $[1, 5]$ and current value 3, its neighboring values are 2 and 4. This allows us to exploit the natural ordering for ordinal variables whilst still ensuring that suggested configurations remain local and only explore *valid* neighboring solutions.

B.3 SUGGESTING NEW ARCHITECTURES

At the start of each generation for the full BG-PBT method, we have to suggest a pool of new architectures. For the first generation, we simply use random sampling across the joint space \mathcal{J} to fill up the initial population. For subsequent generations, we use a combination of BO and random sampling to both leverage information already gained from the architectures and allow sufficient exploration. For the BO, at the start of the i -th generation, we first fit a GP model only in the architecture space \mathcal{Y} , by using the architectures from the $i - 1$ -th generation as the training data. Since these network architectures are trained with different hyperparameters during the generation, we use the *best reward* achieved on each of these architectures as the training targets. We then run BO on this GP to obtain the suggestions for new architectures for the subsequent generation. In practice, to avoid occasional instability in the distillation process, we find it beneficial to select a number of

architectures larger than B : we then start the distillation for all the agents, but use successive halving (Karnin et al., 2013) such that only B agents survive and are distilled for the full budget allocated. By doing so, we trade a modest increase in training steps for greatly improved stability in distillation.

B.4 DETAILS ON TRUST REGIONS

To define trust regions for our time-varying objective, we again consider the most general case where the search space contains both categorical and continuous/ordinal dimensions. Given the configuration $\mathbf{z}_t^* = [\mathbf{h}_t^*, \mathbf{x}_t^*] = \arg \max_{\mathbf{z}_t} (f_t)$ with the best return at time t , we may define the trust region centered around \mathbf{z}_t^* :

$$\text{TR}(\mathbf{z}_T^*) = \begin{cases} \{\mathbf{h} \mid \frac{1}{d_h} \sum_{i=1}^{d_h} \delta(h_i, h_i^*) \leq L_h\} & \text{for categorical } \mathbf{h}_T^* = \{h_i^*\}_{i=1}^{d_h} \\ \{\mathbf{x} \mid |x_i - x_i^*| < \frac{\tilde{\ell}_i}{\prod_{i=1}^{d_x} \tilde{\ell}_i^{d_x}} L_x, 0 \leq x_i \leq 1\} & \text{for continuous or ordinal } \mathbf{x}_T^* = \{x_i^*\}_{i=1}^{d_x}, \end{cases} \quad (8)$$

where $\delta(\cdot, \cdot)$ is the Kronecker delta function, $L_h \in [0, 1]$ is the trust region radius defined in terms of normalized Hamming distance over the categorical variables, L_x is the trust region radius defining a hyperrectangle over the continuous and ordinal variables, and $\{\tilde{\ell}_i = \frac{\ell_i}{\frac{1}{d_x} \sum_{i=1}^{d_x} \ell_i}\}_{i=1}^{d_x}$ are the normalized lengthscales $\{\ell_i\}$ learned by the GP surrogate over the continuous/ordinal dimensions. This means that the more sensitive hyperparameters, i.e. those with smaller learned lengthscales, will automatically be assigned smaller trust region radii.

For the restart of trust regions when either or both of the trust regions defined fall below some pre-defined threshold, we adapt the UCB-based criterion proposed in Wan et al. (2021) to the time-varying setting to re-initialize the population when a restart is triggered. For the i -th restart, we consider a global, auxiliary GP model trained on a subset of observed configurations and returns $D_{i-1}^* = \{\mathbf{z}_j^*, f_j^*\}_{j=1}^i$ and denote $\mu_g(\mathbf{z}; D_{i-1}^*)$ and $\sigma_g^2(\mathbf{z}; D_{i-1}^*)$ as the posterior mean and variance of the auxiliary GP. The new trust region center is given by the configuration $\mathbf{z}_i^{(0)}$ that maximizes the UCB score: $\mathbf{z}_i^{(0)} = \arg \max_{\mathbf{z} \in \mathcal{Z}} \mu_g(\mathbf{z}; D_{i-1}^*) + \sqrt{\beta_i} \sigma_g(\mathbf{z}; D_{i-1}^*)$ where β_i is the UCB trade-off parameter. In the original CASMOPOLITAN, D^* consists of the best configurations in all previous restarts $1, \dots, i-1$, which is invalid for the time-varying setting. Instead, we construct D_{i-1}^* using the following:

$$D_{i-1}^* = \{\mathbf{z}_j^*, \mu_T(\mathbf{z}_j^*)\}_{j=1}^{i-1} \text{ where } \mathbf{z}_j^* = \arg \max_{\mathbf{z}_j \in \mathcal{D}_j} \mu_T(\mathbf{z}_j), \quad (9)$$

where \mathcal{D}_j denotes the set of previous configurations evaluated during the j -th restart and $\mu_T(\cdot)$ denotes the posterior mean of the time-varying GP surrogate *at the present timestep* $t = T$. Thus, instead of simply selecting the configurations of each restart that led to the highest observed reward, we select the configurations that *would have led to the highest reward if they were evaluated now*, according to the GP surrogate. Such a configuration preserves the convergence property of BG-PBT shown in Theorem 3.1 and proven below in App. C.

C THEORETICAL GUARANTEES

C.1 BOUND ON THE MAXIMUM INFORMATION GAIN

We start by deriving the maximum information gain, which extends the result presented in Wan et al. (2021) for the time-varying setting. Note that this result is defined over the number of local restarts I .

Theorem C.1. *Let $\gamma(I; k; V) := \max_{A \subseteq V, |A| \leq I} \frac{1}{2} \log |\mathbf{I} + \sigma^{-2} [k(\mathbf{v}, \mathbf{v}')]_{\mathbf{v}, \mathbf{v}' \in A}|$ be the maximum information gain achieved by sampling I points in a GP defined over a set V with a kernel k . Denote the constant $\eta := \prod_{j=1}^{d_h} n_j$. Then we have, for the time-varying mixed kernel k ,*

$$\gamma(I; k; [\mathcal{H}, \mathcal{X}]) \lesssim \frac{I}{\tilde{N}} \left(\lambda \eta \gamma(I; k_x; \mathcal{X}) + (\eta - 2\lambda) \log I + \sigma_f^{-2} \tilde{N}^3 \omega \right) \quad (10)$$

where the time steps $\{1, \dots, I\}$ are split into I/\tilde{N} blocks of length \tilde{N} , such that the function f_t does not vary significantly within each block.

Proof. Following the proof used in Bogunovic et al. (2016)), we split the time steps $\{1, \dots, I\}$ into I/\tilde{N} blocks of length \tilde{N} , such that within each block the function f_i does not vary significantly. Then, we have that the maximum information gain of the time-varying kernel Bogunovic et al. (2016)) is bounded by

$$\gamma_I \leq \left(\frac{I}{\tilde{N}} + 1 \right) \left(\tilde{\gamma}_{\tilde{N}} + \sigma_f^{-2} \tilde{N}^3 \omega \right)$$

where $\omega \in [0, 1]$ is the forgetting-remembering trade-off parameter, and we consider the kernel for time $1 - k_{time}(t, t') \leq \omega |t - t'|$. We denote $\tilde{\gamma}_{\tilde{N}}$ as the maximum information gain for the time-invariant kernel counterpart in each block length of \tilde{N} .

Next, by using the bounds for the (time-invariant) mixed kernel in Wan et al. (2021) that $\tilde{\gamma}_{\tilde{N}} \leq \mathcal{O}((\lambda\eta + 1 - \lambda)\gamma(I; k_x; \mathcal{X}) + (\eta + 2 - 2\lambda) \log I)$, we get the new time-varying bound $\gamma(I; k; [\mathcal{H}, \mathcal{X}]) \lesssim \frac{I}{\tilde{N}} \left(\lambda\eta\gamma(I; k_x; \mathcal{X}) + (\eta - 2\lambda) \log I + \sigma_f^{-2} \tilde{N}^3 \omega \right)$ where we have suppressed the constant term for simplicity. \square

C.2 PROOF OF THE LOCAL CONVERGENCE IN EACH TRUST REGION

Assumption C.2. *The time-varying objective function $f_t(\mathbf{z})$ is bounded in $[\mathcal{H}, \mathcal{X}]$, i.e. $\exists F_l, F_u \in \mathbb{R} : \forall \mathbf{z} \in [\mathcal{H}, \mathcal{X}], F_l \leq f_t(\mathbf{z}) \leq F_u, \forall t \in [1, \dots, T]$.*

Assumption C.3. *Let us denote L_{\min}^h, L_{\min}^x and L_0^h, L_0^x be the minimum and initial TR lengths for the categorical and continuous variables, respectively. Let us also denote α_s as the shrinking rate of the TRs. The local GP approximates $f_t, \forall t \leq T$ accurately within any TR with length $L^x \leq \max(L_{\min}^x/\alpha_s, L_0^x(\lceil(L_{\min}^h + 1)/\alpha_s\rceil - 1)/L_0^h)$ and $L^h \leq \max(\lceil(L_{\min}^h + 1)/\alpha_s\rceil - 1, \lceil L_0^h L_{\min}^x / (\alpha_s L_0^x) \rceil)$.*

Theorem C.4. *Given Assumptions C.2 & C.3, after a restart, BG-PBT converges to a local maxima after a finite number of iterations or converges to the global maximum.*

Proof. We may apply the same proof by contradiction used in Wan et al. (2021) for our time-varying setting, given the assumptions C.2 and C.3. For completeness, we summarize it below.

We show that our algorithm converges to (1) to a global maximum of f (if does not terminate after a finite number of iterations) or (2) a local maxima of f (if terminated after a finite number of iterations).

Case 1: when $t \rightarrow \infty$ and the TR lengths L^h and L^x have not shrunk below L_{\min}^h and L_{\min}^x . From the algorithm description, the TR is shrunk after `fail_tol` consecutive failures. Thus, if after $N_{\min} = \text{fail_tol} \times m$ iterations where $m = \max(\lceil \log_{\alpha_e}(L_0^h/L_{\min}^h) \rceil, \lceil \log_{\alpha_e}(L_0^x/L_{\min}^x) \rceil)$, there is no success, BG-PBT terminates. This means, for case (1) to occur, BG-PBT needs to have at least one improvement per N_{\min} iterations. Let consider the increasing series $\{f(\mathbf{z}^k)\}_{k=1}^{\infty}$ where $f(\mathbf{z}^k) = \max_{t=(k-1)N_{\min}+1, \dots, kN_{\min}} \{f(\mathbf{z}_t)\}$ and $f(\mathbf{z}_i)$ is the function value at iteration t . Thus, using the monotone convergence theorem (Bibby, 1974), this series converges to the global maximum of the objective function f given that $f(\mathbf{z})$ is bounded (Assumption C.2).

Case 2: when BG-PBT terminates after a finite number of iterations, BG-PBT converges to a local maxima of $f(\mathbf{z})$ given Assumption C.3. Let us remind that BG-PBT terminates when either the continuous TR length $\leq L_{\min}^x$ or the categorical TR length $\leq L_{\min}^h$.

Let L_s be the largest TR length that after being shrunk, the algorithm terminates, i.e., $\lfloor \alpha_s L_s \rfloor \leq L_{\min}^h$.¹ Due to $\lfloor \alpha_s L_s \rfloor \leq \alpha_s L_s < \lfloor \alpha_s L_s \rfloor + 1$, we have $L_s < (L_{\min}^h + 1)/\alpha_s$. Because L_s is an integer, we finally have $L_s \leq \lceil (L_{\min}^h + 1)/\alpha_s \rceil - 1$. This means that $L_s = \lceil (L_{\min}^h + 1)/\alpha_s \rceil - 1$ is the largest TR length that after being shrunk, the algorithm terminates. We may apply a similar argument for the largest TR length (before terminating) for the continuous L_{\min}^x/α_s .

In our mixed space setting, we have two separate trust regions for categorical and continuous variables. When one of the TR reaches its terminating threshold (L_{\min}^x/α_s or $\lceil (L_{\min}^h + 1)/\alpha_s \rceil - 1$), the length of the other one is $(\lceil L_0^h L_{\min}^x / (\alpha_s L_0^x) \rceil)$ or $L_0^x(\lceil (L_{\min}^h + 1)/\alpha_s \rceil - 1)/L_0^h$. Based on Assumption C.3,

¹The operator $\lfloor \cdot \rfloor$ denotes the floor function

the GP can accurately fit a TR with continuous length $L^x \leq \max(L_{\min}^x/\alpha_s, L_0^x(\lceil(L_{\min}^h + 1)/\alpha_s\rceil - 1)/L_0^h)$ and $L^h \leq \max(\lceil(L_{\min}^h + 1)/\alpha_s\rceil - 1, \lceil L_0^h L_{\min}^x / (\alpha_s L_0^x) \rceil)$. Thus, if the current TR center is not a local maxima, BG-PBT can find a new data point whose function value is larger than the function value of current TR center. This process occurs iteratively until a local maxima is reached, and BG-PBT terminates. \square

C.3 PROOF OF THEOREM 3.1

Proof. Under the time-varying setting, at the i -th restart, we first fit the global time-varying GP model on a subset of data $D_{i-1}^* = \{\mathbf{z}_j^*, f(\mathbf{z}_j^*)\}_{j=1}^{i-1}$, where \mathbf{z}_j^* is the local maxima found after the j -th restart, or, a random data point, if the found local maxima after the j -th restart is same as in the previous restart.

Let $\mathbf{z}_i^{**} = \arg \max_{\mathbf{z} \in [\mathcal{H}, \mathcal{X}]} f_i(\mathbf{z})$ ² be the global optimum location at time step i . Let $\mu_{gl}(\mathbf{z}; D_{i-1}^*)$ and $\sigma_{gl}^2(\mathbf{z}; D_{i-1}^*)$ be the posterior mean and variance of the global GP learned from D_{i-1}^* . Then, at the i -th restart, we select the following location $\mathbf{z}_i^{(0)}$ as the initial centre of the new TR:

$$\mathbf{z}_i^{(0)} = \arg \max_{\mathbf{z} \in [\mathcal{H}, \mathcal{X}]} \mu_{gl}(\mathbf{z}; D_{i-1}^*) + \sqrt{\beta_i} \sigma_{gl}(\mathbf{z}; D_{i-1}^*),$$

where β_i is the trade-off parameter in PB2 (Parker-Holder et al., 2020).

We follow Wan et al. (2021) to assume that at the i -th restart, there exists a function $g_i(\mathbf{z})$: (a) lies in the RKHS $\mathcal{G}_k([\mathcal{H}, \mathcal{X}])$ and $\|g_i\|_k^2 \leq B$, (b) shares the same global maximum \mathbf{z}^* with f , and, (c) passes through all the local maxima of f and any data point \mathbf{z}' in $D_{i-1}^* \cup \{\mathbf{z}_i^{(0)}\}$ which are not local maxima (i.e. $g_i(\mathbf{z}') = f(\mathbf{z}'), \forall \mathbf{z}' \in D_{i-1}^* \cup \{\mathbf{z}_i^{(0)}\}$). In other words, the function $g_i(\mathbf{z})$ is a function that passes through the maxima of f whilst lying in the RKHS $\mathcal{G}_k([\mathcal{H}, \mathcal{X}])$ and satisfying $\|g_i\|_k^2 \leq B$.

Using β_i defined in Theorem 2 in Srinivas et al. (2010) for function $g_i, \forall i, \forall z \in [\mathcal{H}, \mathcal{X}]$, we have,

$$\Pr\{|\mu_{gl}(\mathbf{z}; D_{i-1}^*) - g_i(\mathbf{z})| \leq \sqrt{\beta_i} \sigma_{gl}(\mathbf{z}; D_{i-1}^*)\} \geq 1 - \zeta. \quad (11)$$

In particular, with probability $1 - \zeta$, we have that,

$$\mu_{gl}(\mathbf{z}_i^{(0)}; D_{i-1}^*) + \sqrt{\beta_i} \sigma_{gl}(\mathbf{z}_i^{(0)}; D_{i-1}^*) \geq \mu_{gl}(\mathbf{z}_i^{**}; D_{i-1}^*) + \sqrt{\beta_i} \sigma_{gl}(\mathbf{z}_i^{**}; D_{i-1}^*) \geq g_i(\mathbf{z}_i^{**}). \quad (12)$$

Thus, $\forall i$, with probability $1 - \zeta$ we have

$$g_i(\mathbf{z}_i^{**}) - g_i(\mathbf{z}_i^{(0)}) \leq \mu_{gl}(\mathbf{z}_i^{(0)}; D_{i-1}^*) + \sqrt{\beta_i} \sigma_{gl}(\mathbf{z}_i^{(0)}; D_{i-1}^*) - g_i(\mathbf{z}_i^{(0)}) \leq 2\sqrt{\beta_i} \sigma_{gl}(\mathbf{z}_i^{(0)}; D_{i-1}^*).$$

Since $g_i(\mathbf{z}_i^{(0)}) = f(\mathbf{z}_i^{(0)})$, and $g_i(\mathbf{z}_i^{**}) = f(\mathbf{z}_i^{**})$, hence, $f_i(\mathbf{z}_i^{**}) - f_i(\mathbf{z}_i^{(0)}) \leq 2\sqrt{\beta_i} \sigma_{gl}(\mathbf{z}_i^{(0)}; D_{i-1}^*)$ with probability $1 - \zeta$. With \mathbf{z}_i^* as the local maxima found by BG-PBT at the i -th restart. As $f(\mathbf{z}_i^{(0)}) \leq f(\mathbf{z}_i^*)$, we have,

$$f_i(\mathbf{z}_i^{**}) - f_i(\mathbf{z}_i^*) \leq 2\sqrt{\beta_i} \sigma_{gl}(\mathbf{z}_i^{(0)}; D_{i-1}^*). \quad (13)$$

Let $\mathbf{z}_{i,b}$ be the point chosen by our algorithm at iteration i and batch element b , we follow Parker-Holder et al. (2020) to define the time-varying instantaneous regret as $r_{i,b} = f_i(\mathbf{z}_i^{**}) - f_i(\mathbf{z}_{i,b})$. Then, the time-varying batch instantaneous regret over B points is as follows

$$r_i^B = \min_{b \leq B} r_{i,b} = \min_{b \leq B} f_i(\mathbf{z}_i^{**}) - f_i(\mathbf{z}_{i,b}), \forall b \leq B \quad (14)$$

Using Equation (13) and Theorem 2 in Parker-Holder et al. (2020), we bound the cumulative batch regret over I restarts and B parallel agents

$$R_{IB} = \sum_{i=1}^I r_i^B \leq \sqrt{\frac{C_1 I \beta_I}{B}} \gamma(IB; k; [\mathcal{H}, \mathcal{X}]) + 2 \quad (15)$$

²Notationally, at the i -th restart, \mathbf{z}_i^{**} is the global optimum location while \mathbf{z}_i^* is the local maxima found by BG-PBT.

where $C_1 = 32/\log(1+\sigma_f^2)$, β_I is the explore-exploit hyperparameter defined in Theorem 2 in Parker-Holder et al. (2020) and $\gamma(IB; k; [\mathcal{H}, \mathcal{X}]) \lesssim \frac{IB}{N} \left(\lambda\eta\gamma(I; k_x; \mathcal{X}) + (\eta - 2\lambda) \log IB + \sigma_f^{-2} \tilde{N}^3 \omega \right)$ is the maximum information gain defined over the mixed space of categorical and continuous $[\mathcal{H}, \mathcal{X}]$ in the time-varying setting defined in Theorem C.1. □

We note that given Theorem 3.1, if we use the squared exponential kernel over the continuous variables, $\gamma(\tilde{N}B; k; \mathcal{X}) = \mathcal{O}([\log \tilde{N}B]^{d+1})$ (Srinivas et al., 2010), the bound becomes $R_{IB} \leq \sqrt{\frac{C_1 I^2 \beta_I}{N} \left(\lambda\eta [\log \tilde{N}B]^{d+1} + (\eta - 2\lambda) \log IB + \sigma_f^{-2} \tilde{N}^3 \omega \right)} + 2$ where $\tilde{N} \leq I$, $B \ll T$ and $\omega \in [0, 1]$.

D FULL PPO HYPERPARAMETER SEARCH SPACE

We list the full search space for PPO in Table 4. The architecture and hyperparameters form the full 15-dimensional mixed search space. For methods that do not search in the architecture space (e.g., PBT, PB2, random search baselines in \mathcal{Z} , and the partial BG-PBT in Ablation Studies that uses §3.1 only), the last 6 dimensions are fixed to the default architecture used in BRAX: a policy network with 4 hidden layers each containing 32 neurons, and a value network with 5 hidden layers each containing 256 neurons. Spectral normalization is disabled in both networks.

Table 4: The hyperparameters for PPO form a 15-dimensional mixed search space.

Hyperparameter	Type	Range
learning rate	log-uniform	[1e-4, 1e-3]
discount factor (γ)	uniform	[0.9, 0.9999]
entropy coefficient (c)	log-uniform	[1e-6, 1e-1]
unroll length	integer	[5, 15]
reward scaling	uniform	[0.05, 20]
batch size	integer (power of 2)	[32, 1024]
no. updates per epoch	integer	[2, 16]
GAE parameter (λ)	uniform	[0.9, 1]
clipping parameter (ϵ)	uniform	[0.1, 0.4]
π network width	integer (power of 2)	[32, 256]
π network depth	integer	[1, 5]
π use spectral norm	binary	[True, False]
V network width	integer (power of 2)	[32, 256]
V network depth	integer	[1, 5]
V use spectral norm	binary	[True, False]

Table 5: Hyperparameters for BG-PBT inherited from CASMOPOLITAN

Hyperparameter	Value	Description
TR multiplier	1.5	multiplicative factor for each expansion/shrinking of the TR.
succ.tol	3	number of consecutive successes before expanding the TR
fail.tol	10	number of consecutive failures before shrinking the TR
Min. continuous TR radius	0.15	min. TR of the continuous/ordinal variables before restarting
Min. categorical TR radius	0.1	min. TR of the categorical variables before restarting
Init. continuous TR radius	0.4	initial TR of the continuous/ordinal variables
Init. categorical TR radius	1	initial TR of the categorical variables

E IMPLEMENTATION DETAILS

We list the hyperparameters for our method BG-PBT in Table 6. Since BG-PBT uses CASMOPOLITAN BO agent, it also inherits hyperparameters from Wan et al. (2021) which are used in all our experiments (Table 5). We refer the readers to App. B.5 of Wan et al. (2021) which examines the sensitivity of these introduced hyperparameters.

Note that in our current instantiation, we use $\alpha_V = 0$ so we only transfer policy networks across generations, since we found the value function was less informative. We linearly anneal the coefficients for the supervised loss α_V and α_π from their original value to 0 over the course of the distillation phase. This means we smoothly transition to a pure RL loss over the initial part of each new generation.

Table 6: Hyperparameters for BG-PBT.

Hyperparameter	Value	Description
B	8	Population size (number of parallel agents)
q	12.5	% agents replaced each iteration (q)
t_{\max}	150M	Total timesteps
α_{RL}	1	RL weight
α_V	0	Value function weight
α_π	5	Policy weight

Our method is built using the PyTorch version of the BRAX (Freeman et al., 2021) codebase at <https://github.com/google/brax/tree/main/brax>. The codebase is open-sourced under the Apache 2.0 License. The BRAX environments are often subject to change, for full transparency, our evaluation is performed using the 0.10.0 version of the codebase. We ran all our experiments on Nvidia Tesla V100 GPUs and used a single GPU for all experiments.

We note that the PPO baseline used in Table 1 is implemented in a different framework (JAX) to ours, which has some differences in network weight initialization. The hyperparameters for the PPO baseline are tuned via grid-search on a reduced hyperparameter search space (Freeman et al., 2021). Since no hyperparameters were provided for the Hopper environment, we use the default in Freeman et al. (2021).

For all experiments, we use $T_{\max} = 150M$, population size (number of parallel agents) $B = 8$ and $q = 12.5$ (percentage of the agents that are replaced at each PBT iteration – in this case, at each iteration, the worst-performing agent is replaced). For all environments except for Humanoid and Hopper, we use a fixed $t_{\text{ready}} = 1M$. To avoid excessive sensitivity to initialization, at the beginning of training for all PBT-based methods (PB2, PBT and BG-PBT) we initialize with 24 agents and train for t_{ready} steps and choose the top- B agents as the initializing population. For the full BG-PBT, to trigger distillations and hence a new generation, we set a patience of 20 (i.e., if the reward fails to improve after 20 consecutive t_{ready} steps, a new generation is started). We also note that starting new generations can be desirable even if the training has not stalled, and therefore have a second criterion to also start a new generation after 40M steps, and so a new generation is started when either criterion is met (40M steps since last distillation, or 20 consecutive failures in improving the reward). For distillation at the start of every generation (all except initial), at each generation, we also start distillation with 24 agents (4 suggested by BO and the rest from random sampling. See App. B.3 for details) and use successive halving to only distill B of them using the full budget of 30M steps with the rest terminated early. For the Humanoid and Hopper environments, we note that PBT-style methods performed poorly across the board: in particular, on Hopper we notice that agents often learn a sub-optimal mode where it only learns to stand up (hence collecting the reward associating with simply surviving) but not to move. On Humanoid, we find that agents often learn a mode where the humanoid does not use its knee joint – in both cases, the agents seem to learn stable but sub-optimal modes that use fewer degrees-of-freedom than it is capable of exploiting. This behavior was ameliorated by linearly annealing the interval t_{ready} from 5M to 1M as a function of timesteps to not encourage myopic behavior at the start. Since the increase in t_{ready} at the initial stage of training will lead to more exploratory behaviors, we increase the threshold before triggering a new generation at 60M for these two environments.

REFERENCES

- Marcin Andrychowicz, Anton Raichuk, Piotr Stańczyk, Manu Orsini, Sertan Girgin, Raphaël Marinier, Leonard Hussenot, Matthieu Geist, Olivier Pietquin, Marcin Michalski, Sylvain Gelly, and Olivier Bachem. What matters for on-policy deep actor-critic methods? a large-scale study. In *International Conference on Learning Representations*, 2021. URL <https://openreview.net/forum?id=nIAxjsniDzg>.
- Adrià Puigdomènech Badia, Bilal Piot, Steven Kapturowski, Pablo Sprechmann, Alex Vitvitskiy, Zhaohan Daniel Guo, and Charles Blundell. Agent57: Outperforming the atari human benchmark. In *Proceedings of the 37th International Conference on Machine Learning, ICML, 13-18 July, Virtual Event*, volume 119 of *Proceedings of Machine Learning Research*, pp. 507–517. PMLR, 2020. URL <http://proceedings.mlr.press/v119/badia20a.html>.
- Philip Ball, Jack Parker-Holder, Aldo Pacchiano, Krzysztof Choromanski, and Stephen Roberts. Ready policy one: World building through active learning. In *Proceedings of the 37th International Conference on Machine Learning, ICML, 2020*.
- John Bibby. Axiomatisations of the average and a further generalisation of monotonic sequences. *Glasgow Mathematical Journal*, 15(1):63–65, 1974.
- Ilija Bogunovic, Jonathan Scarlett, and Volkan Cevher. Time-varying gaussian process bandit optimization. In *Artificial Intelligence and Statistics*, pp. 314–323, 2016.
- Eric Brochu, Vlad M. Cora, and Nando de Freitas. A tutorial on bayesian optimization of expensive cost functions, with application to active user modeling and hierarchical reinforcement learning. *ArXiv*, abs/1012.2599, 2010.
- Yutian Chen, Aja Huang, Ziyu Wang, Ioannis Antonoglou, Julian Schrittwieser, David Silver, and Nando de Freitas. Bayesian optimization in AlphaGo. *CoRR*, abs/1812.06855, 2018.
- John D Co-Reyes, Yingjie Miao, Daiyi Peng, Esteban Real, Quoc V Le, Sergey Levine, Honglak Lee, and Aleksandra Faust. Evolving reinforcement learning algorithms. In *International Conference on Learning Representations*, 2021. URL <https://openreview.net/forum?id=0XXpJ40tjW>.
- Karl Cobbe, Oleg Klimov, Chris Hesse, Taehoon Kim, and John Schulman. Quantifying generalization in reinforcement learning. In Kamalika Chaudhuri and Ruslan Salakhutdinov (eds.), *Proceedings of the 36th International Conference on Machine Learning*, volume 97 of *Proceedings of Machine Learning Research*, pp. 1282–1289. PMLR, 09–15 Jun 2019. URL <https://proceedings.mlr.press/v97/cobbe19a.html>.
- Karl Cobbe, Christopher Hesse, Jacob Hilton, and John Schulman. Leveraging procedural generation to benchmark reinforcement learning, 2020.
- Wojciech Czarnecki, Siddhant Jayakumar, Max Jaderberg, Leonard Hasenclever, Yee Whye Teh, Nicolas Heess, Simon Osindero, and Razvan Pascanu. Mix & match agent curricula for reinforcement learning. In *Proceedings of the 35th International Conference on Machine Learning*, volume 80 of *Proceedings of Machine Learning Research*, pp. 1087–1095. PMLR, 10–15 Jul 2018.
- Valentin Dalibard and Max Jaderberg. Faster improvement rate population based training. *CoRR*, abs/2109.13800, 2021.
- Michael Dennis, Natasha Jaques, Eugene Vinitsky, Alexandre M. Bayen, Stuart Russell, Andrew Critch, and Sergey Levine. Emergent complexity and zero-shot transfer via unsupervised environment design. In *Advances in Neural Information Processing Systems 33: December 6-12, virtual*, 2020. URL <https://proceedings.neurips.cc/paper/2020/hash/985e9a46e10005356bbaf194249f6856-Abstract.html>.
- Logan Engstrom, Andrew Ilyas, Shibani Santurkar, Dimitris Tsipras, Firdaus Janoos, Larry Rudolph, and Aleksander Madry. Implementation matters in deep RL: A case study on PPO and TRPO. In *8th International Conference on Learning Representations, ICLR, Addis Ababa, Ethiopia, April 26-30*. OpenReview.net, 2020. URL <https://openreview.net/forum?id=r1etN1rtPB>.

- David Eriksson, Michael Pearce, Jacob Gardner, Ryan D Turner, and Matthias Poloczek. Scalable global optimization via local bayesian optimization. *Advances in Neural Information Processing Systems*, 32, 2019.
- Sebastian Flennerhag, Yannick Schroecker, Tom Zahavy, Hado van Hasselt, David Silver, and Satinder Singh. Bootstrapped meta-learning. In *arxiv*, 2021.
- Peter I Frazier. A tutorial on Bayesian optimization. *arXiv preprint arXiv:1807.02811*, 2018.
- C. Daniel Freeman, Erik Frey, Anton Raichuk, Sertan Girgin, Igor Mordatch, and Olivier Bachem. Brax - a differentiable physics engine for large scale rigid body simulation, 2021. URL <http://github.com/google/brax>.
- Yonggan Fu, Zhongzhi Yu, Yongan Zhang, and Yingyan Lin. Auto-agent-distiller: Towards efficient deep reinforcement learning agents via neural architecture search. *arXiv preprint arXiv:2012.13091*, 2020.
- Hiroki Furuta, Tatsuya Matsushima, Tadashi Kozuno, Yutaka Matsuo, Sergey Levine, Ofir Nachum, and Shixiang Shane Gu. Policy information capacity: Information-theoretic measure for task complexity in deep reinforcement learning. In *International Conference on Machine Learning*, 2021.
- Peter Henderson, Riashat Islam, Philip Bachman, Joelle Pineau, Doina Precup, and David Meger. Deep reinforcement learning that matters. In *Proceedings of the Thirty-Second AAAI Conference on Artificial Intelligence, (AAAI)*, pp. 3207–3214. AAAI Press, 2018. URL <https://www.aaai.org/ocs/index.php/AAAI/AAAI18/paper/view/16669>.
- Maximilian Igl, Gregory Farquhar, Jelena Luketina, Wendelin Boehmer, and Shimon Whiteson. Transient non-stationarity and generalisation in deep reinforcement learning. In *International Conference on Learning Representations*, 2021. URL <https://openreview.net/forum?id=Qun8fv4qSby>.
- Sergio Izquierdo, Julia Guerrero-Viu, Sven Hauns, Guilherme Miotto, Simon Schrodi, André Biedenkapp, Thomas Elsken, Difan Deng, Marius Lindauer, and Frank Hutter. Bag of baselines for multi-objective joint neural architecture search and hyperparameter optimization. In *8th ICML Workshop on Automated Machine Learning (AutoML)*, 2021.
- Max Jaderberg, Valentin Dalibard, Simon Osindero, Wojciech M. Czarnecki, Jeff Donahue, Ali Razavi, Oriol Vinyals, Tim Green, Iain Dunning, Karen Simonyan, Chrisantha Fernando, and Koray Kavukcuoglu. Population based training of neural networks. *CoRR*, abs/1711.09846, 2017.
- Max Jaderberg, Wojciech M. Czarnecki, Iain Dunning, Luke Marris, Guy Lever, Antonio Garcia Castañeda, Charles Beattie, Neil C. Rabinowitz, Ari S. Morcos, Avraham Ruderman, Nicolas Sonnerat, Tim Green, Louise Deason, Joel Z. Leibo, David Silver, Demis Hassabis, Koray Kavukcuoglu, and Thore Graepel. Human-level performance in 3d multiplayer games with population-based reinforcement learning. *Science*, 364(6443):859–865, 2019.
- Kevin Jamieson and Ameet Talwalkar. Non-stochastic best arm identification and hyperparameter optimization. In Arthur Gretton and Christian C. Robert (eds.), *Proceedings of the 19th International Conference on Artificial Intelligence and Statistics*, volume 51 of *Proceedings of Machine Learning Research*, pp. 240–248, Cadiz, Spain, 09–11 May 2016. PMLR. URL <https://proceedings.mlr.press/v51/jamieson16.html>.
- Minqi Jiang, Michael Dennis, Jack Parker-Holder, Jakob Foerster, Edward Grefenstette, and Tim Rocktäschel. Replay-guided adversarial environment design. In *Advances in Neural Information Processing Systems*. 2021.
- Dmitry Kalashnikov, Alex Irpan, Peter Pastor, Julian Ibarz, Alexander Herzog, Eric Jang, Deirdre Quillen, Ethan Holly, Mrinal Kalakrishnan, Vincent Vanhoucke, and Sergey Levine. Scalable deep reinforcement learning for vision-based robotic manipulation. In Aude Billard, Anca Dragan, Jan Peters, and Jun Morimoto (eds.), *Proceedings of The 2nd Conference on Robot Learning*, volume 87 of *Proceedings of Machine Learning Research*, pp. 651–673. PMLR, 29–31 Oct 2018. URL <https://proceedings.mlr.press/v87/kalashnikov18a.html>.

- Kirthevasan Kandasamy, Willie Neiswanger, Jeff Schneider, Barnabas Poczos, and Eric P Xing. Neural architecture search with bayesian optimisation and optimal transport. *Advances in neural information processing systems*, 31, 2018.
- Zohar Karnin, Tomer Koren, and Oren Somekh. Almost optimal exploration in multi-armed bandits. In Sanjoy Dasgupta and David McAllester (eds.), *Proceedings of the 30th International Conference on Machine Learning*, volume 28 of *Proceedings of Machine Learning Research*, pp. 1238–1246, Atlanta, Georgia, USA, 17–19 Jun 2013. PMLR. URL <https://proceedings.mlr.press/v28/karnin13.html>.
- Marius Lindauer, Katharina Eggenberger, Matthias Feurer, André Biedenkapp, Difan Deng, Carolin Benjamins, Tim Ruhkopf, René Sass, and Frank Hutter. Smac3: A versatile bayesian optimization package for hyperparameter optimization. *Journal of Machine Learning Research*, 23(54):1–9, 2022.
- Hanxiao Liu, Karen Simonyan, and Yiming Yang. DARTS: Differentiable architecture search. In *International Conference on Learning Representations*, 2019.
- Siqi Liu, Guy Lever, Zhe Wang, Josh Merel, S. M. Ali Eslami, Daniel Hennes, Wojciech M. Czarnecki, Yuval Tassa, Shayegan Omidshafiei, Abbas Abdolmaleki, Noah Y. Siegel, Leonard Hasenclever, Luke Marris, Saran Tunyasuvunakool, H. Francis Song, Markus Wulfmeier, Paul Muller, Tuomas Haarnoja, Brendan D. Tracey, Karl Tuyls, Thore Graepel, and Nicolas Heess. From motor control to team play in simulated humanoid football. *CoRR*, abs/2105.12196, 2021.
- Yingjie Miao, Xingyou Song, Daiyi Peng, Summer Yue, Eugene Brevdo, and Aleksandra Faust. RL-DARTS: differentiable architecture search for reinforcement learning. *CoRR*, abs/2106.02229, 2021. URL <https://arxiv.org/abs/2106.02229>.
- Volodymyr Mnih, Koray Kavukcuoglu, David Silver, Alex Graves, Ioannis Antonoglou, Daan Wierstra, and Martin A. Riedmiller. Playing atari with deep reinforcement learning. *CoRR*, abs/1312.5602, 2013.
- Ted Moskowitz, Jack Parker-Holder, Aldo Pacchiano, and Michael Arbel. Deep reinforcement learning with dynamic optimism. In *Advances in Neural Information Processing Systems*. 2021.
- V Nguyen, SB Orbell, Dominic T Lennon, Hyungil Moon, Florian Vigneau, Leon C Camenzind, Liuqi Yu, Dominik M Zumbühl, G Andrew D Briggs, Michael A Osborne, et al. Deep reinforcement learning for efficient measurement of quantum devices. *npj Quantum Information*, 7(1):1–9, 2021a.
- Vu Nguyen, Tam Le, Makoto Yamada, and Michael A Osborne. Optimal transport kernels for sequential and parallel neural architecture search. In *International Conference on Machine Learning*, pp. 8084–8095. PMLR, 2021b.
- Junhyuk Oh, Matteo Hessel, Wojciech M. Czarnecki, Zhongwen Xu, Hado van Hasselt, Satinder Singh, and David Silver. Discovering reinforcement learning algorithms. In *Advances in Neural Information Processing Systems 33: Annual Conference on Neural Information Processing Systems 2020, NeurIPS 2020, December 6-12, 2020, virtual*, 2020. URL <https://proceedings.neurips.cc/paper/2020/hash/0b96d81f0494fde5428c7aea243c9157-Abstract.html>.
- Kei Ota, Devesh K. Jha, and Asako Kanezaki. Training larger networks for deep reinforcement learning, 2021.
- Daniel Park, Jascha Sohl-Dickstein, Quoc Le, and Samuel Smith. The effect of network width on stochastic gradient descent and generalization: an empirical study. In Kamalika Chaudhuri and Ruslan Salakhutdinov (eds.), *Proceedings of the 36th International Conference on Machine Learning*, volume 97 of *Proceedings of Machine Learning Research*, pp. 5042–5051. PMLR, 09–15 Jun 2019. URL <https://proceedings.mlr.press/v97/park19b.html>.
- Jack Parker-Holder, Vu Nguyen, and Stephen J Roberts. Provably efficient online hyperparameter optimization with population-based bandits. In H. Larochelle, M. Ranzato, R. Hadsell, M. F. Balcan, and H. Lin (eds.), *Advances in Neural Information Processing Systems*, volume 33, pp. 17200–17211. Curran Associates, Inc., 2020. URL <https://proceedings.neurips.cc/paper/2020/file/c7af0926b294e47e52e46cfebe173f20-Paper.pdf>.

- Jack Parker-Holder, Aldo Pacchiano, Krzysztof Choromanski, and Stephen Roberts. Effective diversity in population-based reinforcement learning. In *Advances in Neural Information Processing Systems 33*. 2020.
- Jack Parker-Holder, Vu Nguyen, Shaan Desai, and S Roberts. Tuning mixed input hyperparameters on the fly for efficient population based autoRL. In A. Beygelzimer, Y. Dauphin, P. Liang, and J. Wortman Vaughan (eds.), *Advances in Neural Information Processing Systems*, 2021. URL <https://openreview.net/forum?id=no-Jsrx9ytl>.
- Jack Parker-Holder, Raghu Rajan, Xingyou Song, André Biedenkapp, Yingjie Miao, Theresa Eimer, Baohe Zhang, Vu Nguyen, Roberto Calandra, Aleksandra Faust, Frank Hutter, and Marius Lindauer. Automated reinforcement learning (autorl): A survey and open problems. *CoRR*, abs/2201.03916, 2022.
- Supratik Paul, Vitaly Kurin, and Shimon Whiteson. Fast efficient hyperparameter tuning for policy gradient methods. In *Advances in Neural Information Processing Systems*, volume 32, 2019.
- C. E. Rasmussen and C. K. I. Williams. *Gaussian Processes for Machine Learning*. MIT Press, 2006.
- Binxin Ru, Xingchen Wan, Xiaowen Dong, and Michael Osborne. Interpretable neural architecture search via bayesian optimisation with weisfeiler-lehman kernels. *International Conference on Learning Representations*, 2021.
- John Schulman, Sergey Levine, Pieter Abbeel, Michael Jordan, and Philipp Moritz. Trust region policy optimization. In Francis Bach and David Blei (eds.), *Proceedings of the 32nd International Conference on Machine Learning*, volume 37 of *Proceedings of Machine Learning Research*, pp. 1889–1897, Lille, France, 07–09 Jul 2015. PMLR. URL <https://proceedings.mlr.press/v37/schulman15.html>.
- John Schulman, Filip Wolski, Prafulla Dhariwal, Alec Radford, and Oleg Klimov. Proximal policy optimization algorithms, 2017.
- Bobak Shahriari, Kevin Swersky, Ziyu Wang, Ryan P Adams, and Nando de Freitas. Taking the human out of the loop: A review of Bayesian optimization. *Proceedings of the IEEE*, 104(1): 148–175, 2016.
- David Silver, Julian Schrittwieser, Karen Simonyan, Ioannis Antonoglou, Aja Huang, Arthur Guez, Thomas Hubert, Lucas baker, Matthew Lai, Adrian Bolton, Yutian Chen, Timothy P. Lillicrap, Fan Hui, L. Sifre, George van den Driessche, Thore Graepel, and Demis Hassabis. Mastering the game of go without human knowledge. *Nature*, 550:354–359, 2017.
- David Silver, Satinder Singh, Doina Precup, and Richard S. Sutton. Reward is enough. *Artificial Intelligence*, 299:103535, 2021. ISSN 0004-3702. doi: <https://doi.org/10.1016/j.artint.2021.103535>.
- Niranjan Srinivas, Andreas Krause, Sham Kakade, and Matthias Seeger. Gaussian process optimization in the bandit setting: No regret and experimental design. In *Proceedings of the 27th International Conference on Machine Learning*, pp. 1015–1022, 2010.
- Adam Stooke, Anuj Mahajan, Catarina Barros, Charlie Deck, Jakob Bauer, Jakub Sygnowski, Maja Trebacz, Max Jaderberg, Michaël Mathieu, Nat McAleese, Nathalie Bradley-Schmieg, Nathaniel Wong, Nicolas Porcel, Roberta Raileanu, Steph Hughes-Fitt, Valentin Dalibard, and Wojciech Marian Czarnecki. Open-ended learning leads to generally capable agents. *arXiv preprint arXiv:2107.12808*, 2021.
- Richard S. Sutton and Andrew G. Barto. *Reinforcement Learning: An Introduction*. The MIT Press, second edition, 2018.
- Yunhao Tang and Krzysztof Choromanski. Online hyper-parameter tuning in off-policy learning via evolutionary strategies. *CoRR*, abs/2006.07554, 2020. URL <https://arxiv.org/abs/2006.07554>.

- Oriol Vinyals, Igor Babuschkin, Wojciech M. Czarnecki, Michaël Mathieu, Andrew Dudzik, Junyoung Chung, David H. Choi, Richard Powell, Timo Ewalds, Petko Georgiev, Junhyuk Oh, Dan Horgan, Manuel Kroiss, Ivo Danihelka, Aja Huang, L. Sifre, Trevor Cai, John P. Agapiou, Max Jaderberg, Alexander Sasha Vezhnevets, Rémi Leblond, Tobias Pohlen, Valentin Dalibard, David Budden, Yury Sulsky, James Molloy, Tom Le Paine, Caglar Gulcehre, Ziyun Wang, Tobias Pfaff, Yuhuai Wu, Roman Ring, Dani Yogatama, Dario Wünsch, Katrina McKinney, Oliver Smith, Tom Schaul, Timothy P. Lillicrap, Koray Kavukcuoglu, Demis Hassabis, Chris Apps, and David Silver. Grandmaster level in starcraft ii using multi-agent reinforcement learning. *Nature*, pp. 1–5, 2019.
- Xingchen Wan, Vu Nguyen, Huong Ha, Binxin Ru, Cong Lu, and Michael A. Osborne. Think global and act local: Bayesian optimisation over high-dimensional categorical and mixed search spaces. In Marina Meila and Tong Zhang (eds.), *Proceedings of the 38th International Conference on Machine Learning*, volume 139 of *Proceedings of Machine Learning Research*, pp. 10663–10674. PMLR, 18–24 Jul 2021. URL <https://proceedings.mlr.press/v139/wan21b.html>.
- Xingchen Wan, Binxin Ru, Pedro M Esparançã, and Fabio Maria Carlucci. Approximate neural architecture search via operation distribution learning. In *Proceedings of the IEEE/CVF Winter Conference on Applications of Computer Vision*, pp. 2377–2386, 2022.
- Rui Wang, Joel Lehman, Jeff Clune, and Kenneth O. Stanley. Paired open-ended trailblazer (poet): Endlessly generating increasingly complex and diverse learning environments and their solutions. *ArXiv*, abs/1901.01753, 2019.
- Rui Wang, Joel Lehman, Aditya Rawal, Jiale Zhi, Yulun Li, Jeff Clune, and Kenneth O. Stanley. Enhanced poet: Open-ended reinforcement learning through unbounded invention of learning challenges and their solutions. In *ICML*, 2020.
- Colin White, Willie Neiswanger, and Yash Savani. Bananas: Bayesian optimization with neural architectures for neural architecture search. *AAAI*, 1(2):4, 2021.
- Jie Xu, Miles Macklin, Viktor Makoviyshuk, Yashraj Narang, Animesh Garg, Fabio Ramos, and Wojciech Matusik. Accelerated policy learning with parallel differentiable simulation. In *International Conference on Learning Representations*, 2022. URL <https://openreview.net/forum?id=ZSKRQMvttc>.
- Zhongwen Xu, Hado van Hasselt, and David Silver. Meta-gradient reinforcement learning. In *Advances in Neural Information Processing Systems 31: NeurIPS, December 3-8, Montréal, Canada*, pp. 2402–2413, 2018. URL <https://proceedings.neurips.cc/paper/2018/hash/2715518c875999308842e3455eda2fe3-Abstract.html>.
- Ya-xiang Yuan. A review of trust region algorithms for optimization. *ICM99: Proceedings of the Fourth International Congress on Industrial and Applied Mathematics*, 09 1999.
- Tom Zahavy, Zhongwen Xu, Vivek Veeriah, Matteo Hessel, Junhyuk Oh, Hado van Hasselt, David Silver, and Satinder Singh. A self-tuning actor-critic algorithm. In *Advances in Neural Information Processing Systems*, 2020.
- Baohe Zhang, Raghu Rajan, Luis Pineda, Nathan Lambert, André Biedenkapp, Kurtland Chua, Frank Hutter, and Roberto Calandra. On the importance of hyperparameter optimization for model-based reinforcement learning. In *Proceedings of The 24th International Conference on Artificial Intelligence and Statistics*, 2021.